

RESEARCH ARTICLE

[View Article Online](#)
[View Journal](#)

Cite this: DOI: 10.1039/d2mo00257d

Plasma extracellular vesicles microRNA-208b-3p and microRNA-143-3p as novel biomarkers for sudden cardiac death prediction in acute coronary syndrome†

Shuainan Huang,^{‡a} Jiahui Zhang,^{‡b} Hua Wan,^{‡c} Kang Wang,^a Jiayi Wu,^a Yue Cao,^{ib a} Li Hu,^a Yanfang Yu,^a Hao Sun,^b Youjia Yu,^{ib *a} Jie Wang^{*a} and Feng Chen^{ib *ad}

Acute coronary syndrome (ACS) occurs as a result of myocardial ischemia that can give rise to a variety of acute cardiovascular events, including arrhythmia, heart failure and sudden cardiac death (SCD). Currently, there are challenges and insufficient innovations regarding early diagnosis and therapeutic approaches within ACS patients experiencing SCD. Plasma extracellular vesicles (EVs) might serve as biomarkers of many diseases depending on the biological molecules of their cargo, such as miRNAs. This study aims to identify the plasma EVs containing miRNAs as novel biomarkers for the prediction of SCD in ACS patients. A total of 39 ACS patients experiencing SCD and 39 healthy control individuals (HC) were enrolled, among which 9 samples in each group were randomly selected as testing groups for miRNA sequencing in plasma EVs, and the remaining samples were assigned to the validation group. The top 10 significant expression miRNAs were verified by the real-time quantitative polymerase chain reaction. Upregulation of miR-208b-3p, miR-143-3p, miR-145-3p and miR-152-3p, and down-regulation of miR-183-5p were further validated in the validation group. Spearman's correlation analysis and the receiver operating characteristic (ROC) curve showed that both miR-208b-3p and miR-143-3p levels were positively correlated with myoglobin (MYO), and their predictive power for SCD was confirmed. In conclusion, our findings indicate that plasma EVs miR-208b-3p and miR-143-3p may serve as promising biomarkers in predicting SCD in patients with ACS, as well as postmortem forensic diagnosis of the cause of death due to ACS.

Received 19th September 2022,
Accepted 8th December 2022

DOI: 10.1039/d2mo00257d

rsc.li/molomics

1 Introduction

Sudden cardiac death (SCD) is defined as the unexpected acute death from cardiac causes within one hour of the onset of symptoms or during sleep in a person who is previously stable.¹ SCD is a major cause of death, accounting for approximately 50% of all cardiovascular deaths² and causes 300 000 to 400 000

deaths in the United States every year.³ The incidence of SCD is 41.84/100 000 persons per year in China.⁴ Eighty percent of SCD cases are caused by coronary heart disease (CHD) and its complications, while the rest are caused by cardiomyopathy, heart valve disease, congenital heart disease, pulmonary embolism, *etc.*⁵

Acute coronary syndrome (ACS) is the most serious subset of CHD and is life-threatening, affecting over a million people per year.⁶ ACS occurs as a result of myocardial ischemia and includes ST-segment elevation myocardial infarction (STEMI), non-ST-segment elevation myocardial infarction (NSTEMI) and unstable angina (UA).⁷ ACS can give rise to a variety of acute cardiovascular events, including arrhythmia, heart failure and SCD.⁸ At present, few biomarkers can be used as prognostic indicators of ACS, partially due to the limitation in the mechanism studies of ACS.⁹ To date, identification of the cause of death in SCD cases also remains one of the most challenging subjects in forensic practice due to the lack of biomarkers.⁴ Hence, there is an urgent need for exploring novel functional

^a Department of Forensic Medicine, Nanjing Medical University, 101 Longmian Ave, Nanjing, Jiangsu, 211166, P. R. China. E-mail: fchen@njmu.edu.cn, jwang2019@126.com, yuyoujia@njmu.edu.cn; Tel: +86-25-86869342

^b The First Affiliated Hospital of Nanjing Medical University, Nanjing, Jiangsu, 211166, P. R. China

^c Department of Health Management, Sir Run Run Hospital, Nanjing Medical University, Nanjing 211166, China

^d Key Laboratory of Targeted Intervention of Cardiovascular Disease, Collaborative Innovation Center for Cardiovascular Disease Translational Medicine, Nanjing Medical University, Nanjing, Jiangsu, 211166, People's Republic of China

† Electronic supplementary information (ESI) available. See DOI: <https://doi.org/10.1039/d2mo00257d>

‡ These authors contributed equally to this work.

biomarkers for the prediction of SCD in patients with ACS and for forensic identification of SCD.

Extracellular vesicles (EVs) are nanometer-sized (50–150 nm) lipid membrane vesicles secreted from all kinds of cell types into the extracellular space.¹⁰ Multiple body fluids, including urine, blood and amniotic fluid, contain abundant EVs.¹¹ EVs can transfer a large number of proteins, lipids, RNA, microRNAs (miRNAs), and other substances from donor cells to recipient cells.^{10,12} It has been shown that EVs are important carriers of bioactive molecules and play essential roles in cell–cell communication, cell growth, cell migration, angiogenesis and immune response during the progression of multiple diseases, prompting their application as early detection and treatment response biomarkers.^{13–17} The potential of plasma and serum EVs containing miRNAs as diagnostic biomarkers for cardiovascular diseases has been demonstrated.¹⁸ For instance, serum EVs containing miR-133a can be used as biomarkers for cardiomyocyte death and may contribute to the development of cardiovascular diseases.¹⁹ In addition, owing to the stable double membrane structure, EVs are protected from being degraded by humoral enzymes and they maintain their integrity in body fluids.²⁰ Therefore, EVs are considered to be ideal diagnostic carriers for cardiovascular diseases.²¹

MiRNAs are small noncoding RNAs (20–24 nucleotides) that regulate post-transcriptional gene expression and play an important role in a broad range of biological processes.^{22,23} To date, studies have highlighted the important roles of miRNAs in the pathological development of multiple cardiovascular diseases.²⁴ Preliminary evidence has indicated that miRNAs may play essential roles in the pathogenesis of ACS. Previous research has reported that miR-941 may be a potential biomarker of STEMI since it is relatively higher in ACS patients with STEMI, and can be used to predict the severity and progression of CHD.²⁵ Platelet miR-142-3p is over-expressed in ACS and shows great potential to be a prognostic biomarker in modeling the risk of ACS.²⁶ In addition, plasma miR-150-5p, miR-29a-3p and miR-30a-5p may have the potential to predict SCD risk and regulate pathways important for remodeling.²⁷ Nevertheless, the mechanisms or roles of miRNAs in paracrine crosstalk during the progression of ACS or SCD remain largely unknown.

In this study, a total of 39 patients with ACS experiencing SCD and 39 healthy control individuals (HC) were studied to identify EV biomarkers that could predict SCD. By profiling the miRNA content in EVs derived from plasma and validating the expressions of differential miRNAs in SCD patients and HC, plasma EVs miR-208b-3p and miR-143-3p were ultimately identified as reliable biomarkers for the prediction of SCD. Furthermore, these data may also contribute to forensic diagnostic purposes.^{28,29}

2 Materials and methods

2.1 Subject information and plasma sample collection

A total of 39 ACS patients experiencing SCD and 39 HC were included in this study. The inclusion criteria were as follows: (1) patients above 18 years old; (2) patients diagnosed with ACS in accordance with the 2019 ACC/AHA Guideline; (3) patients

with cardiopulmonary arrest. The exclusion criteria were as follows: (I) malignant tumors, immune system diseases and blood system diseases; (II) stroke; (III) previous coronary artery bypass surgery; (IV) chronic obstructive pulmonary disease or complicated with pulmonary infection; (V) history of gastric ulcer or gastrointestinal bleeding; (VI) chronic or acute renal impairment; and (VII) inorganic cardiopathy. HC who underwent physical examination in the Sir Run Run Hospital were enrolled in the HC group. The inclusion criteria of HC were as follows: (1) above 18 years old; (2) no history of serious diseases; (3) physical examination reports showed no significant abnormalities in liver or kidney function. The medical history, laboratory examination and echocardiographic results of SCD patients were collected after admission. Experiments were carried out under the approval of the ethics committee of the Jiangsu Province Hospital and the Sir Run Run Hospital (No. 2021-SR-320 and 2021-SR-003). Signed written informed consents were obtained from all participants or their dependents.

For each patient, 10 mL of venous blood was collected using the dipotassium ethylenediaminetetraacetic acid (EDTA-K₂) anticoagulant tube (BD Vacutainer, USA) immediately after admission. For HC, the fasting blood samples were collected in the morning. All the samples were kept at 4 °C and processed within 1 h after collection. Whole blood was centrifuged at 1500g at 4 °C for 15 min. The supernatant platelet-free plasma was collected and aliquoted into clean 1.5 mL Eppendorf tubes and stored at –80 °C before use. We randomly selected 9 SCD patients and 9 HC as testing groups. Every 3 samples were randomly and equally mixed and used for miRNA sequencing. The rest 30 SCD patients and 30 HC were assigned to validation groups.

2.2 EV isolation

EVs were isolated by ultracentrifugation, 2 mL of plasma was thawed at 37 °C in a water bath, diluted with phosphate buffered saline (PBS) to 10 mL, and pre-cleared by centrifugation at 2000g, at 4 °C for 20 min. The supernatant was centrifuged at 10 000g for 30 min at 4 °C to remove cells and cell debris, followed by filtration through a 0.22 µm filter (Millipore, USA). The supernatant was then ultracentrifuged at 200 000g for 2 h at 4 °C using 10.4 mL Centrifuge Tubes, 70.1 Ti fixed angle rotor, Beckman L-100XP Ultracentrifuge and Beckman Coulter.³⁰ The supernatant was discarded and the pellets were resuspended in 500 µL PBS and then mixed with PBS to a final volume of 10 mL and ultracentrifuged for 2 h at 200 000g at 4 °C. The EVs (pellets) were resuspended with PBS to a final volume of 100 µL.

2.3 Extraction of total RNA

EVs resuspended with 100 µL PBS were added to 1 mL of Trizol reagent (Thermo Fisher Scientific, USA), mixed thoroughly, and then immediately incubated for 5 min at room temperature (RT), followed by mixing with 200 µL of chloroform. After incubation for 15 min at RT, the sample was centrifuged at 12 000g at 4 °C for 15 min. The 500 µL supernatant was placed in a new 1.5 mL RNA-free centrifuge tube in which 500 µL of isopropanol was mixed. This mixture was left at –20 °C for

20 min and then centrifuged at 12 000g for 10 min at 4 °C. The supernatant was discarded, and 1 mL of 75% ethanol was added to rinse the precipitate, followed by centrifugation for 5 min at 12 000g at 4 °C, after which the precipitate was washed again using the procedure of the last step. Then, 40 µL of diethyl pyrocarbonate (DEPC) water was added to dissolve the RNA and then stored at –80 °C until use. The RNA concentration determination was accomplished using NanoDrop 2000 (Thermo Fisher Scientific, USA).

2.4 Nanoparticle tracking analysis

The particle size and concentration analysis of EVs were performed by nanoparticle tracking analysis (NTA) with Zeta-View PMX 110 (Particle Metrix, Meerbusch, Germany) and the corresponding software ZetaView 8.04.02 SP2.³¹ The EVs were diluted in PBS to the concentration of 10⁷ particles per mL. Laser scattering microscopy (LSM) images were recorded using Particle Metrix system (Particle Metrix, Meerbusch, Germany).

2.5 Transmission electron microscopy

For transmission electron microscopy (TEM) analysis, the following procedure was employed: 1 µL of EVs were diluted to 20 µL using PBS and added onto formvar-carbon coated copper grids for 10 min. The grids were washed three times with ddH₂O and the excess solution was removed using a filter paper. The grids were then negatively stained with 30 µL of 2% uranyl acetate and incubated for 10 min. Micrographs of EVs were obtained on an FEI Tecnai G2 TEM (FEI, USA).

2.6 Western blotting

For Western blotting, EVs were lysed with lysis buffer (10 mM Tris pH 7.5, 150 mM NaCl, 0.5 mM EDTA, 0.1% SDS, 1% deoxycholate, 1% TritonX-100) supplemented with PMSF (1 µM) and heated at 100 °C for 10 min. Proteins of EVs (20 µg from each sample) were separated by 8%–12% sodium dodecyl sulfate polyacrylamide gel electrophoresis (SDS-PAGE) and transferred onto polyvinylidene fluoride (PVDF) membranes. After blocking with 5% skim milk at RT for 1 h, the membranes were incubated with primary antibodies including anti-CD9 antibody (#ab92726, 1:1000; Abcam, UK), anti-CD63 antibody (#25682-1-AP, 1:500; Proteintech, USA), anti-CD81 antibody (#ab109201, 1:1,000; Abcam, UK), anti-Hsp70 antibody (#610607, 1:1000; BD Biosciences, USA) and anti-Calnexin antibody (#ET1611-86, 1:1000; HUABIO, China) overnight at 4 °C and then incubated with horseradish peroxidase (HRP) conjugated anti-rabbit (#BS13278, 1:8000; Biogot Technology, China) or anti-mouse (#BS12478, 1:8000; Biogot Technology, China) secondary antibodies for 1 h at RT. The immunoreactive bands were imaged using a luminescent imaging system (Tanon, China).

2.7 MicroRNA sequencing and data analysis

Approximately 10 ng of RNA from each sample was used for the preparation of a small RNA library according to the manufacturer's instructions of TruSeq Small RNA Sample Prep Kits

(Illumina, San Diego, USA). The single-end sequencing (1 × 50bp) was performed on the Illumina HiSeq 2500 platform as described previously,³² and then, the data were analyzed using ACGT101-miR software (LC Sciences, Houston, Texas, USA) to remove junk reads, adapter sequences, reads less than 18 nt, reads more than 26 nt, and common RNA families (rRNA, tRNA, snRNA, and snoRNA),³³ followed by comparing with the Rfam database (<https://rfam.xfam.org/>) and the Repbase database (<https://www.girinst.org/education/index.html>). We used FastQC software to conduct quality control analysis.³⁴ The overall reads for each sample were 20 M. Student's *t*-test was used to screen for significantly different miRNAs. MiRNAs were deemed significantly differentially expressed if (I) *P* value < 0.05; (II) fold change ≥ 2 (upregulated miRNAs) or fold change ≤ 0.5 (downregulated miRNAs); (III) average raw value of the group with a higher raw value among SCD and HC groups > 100.

2.8 Reverse transcription and real-time quantitative polymerase chain reaction

After the RNA concentration was determined, a reverse transcription kit (Takara, Japan) was used for the synthesis of cDNA according to the manufacturer's instructions. Real-time quantitative polymerase chain reaction (RT-qPCR) was used to detect miRNA expression. The total reaction volume was 10 µL, including 1 µL of cDNA, 5 µL of 2 × qPCR MasterMix and 0.4 µL of primers. Each experiment was repeated three times using a CFX Connect TM Real-Time PCR Detection System (Bio-Rad). With U6 as the internal reference, the comparative Ct ($\Delta\Delta C_t$) method was used to quantify relative miRNA expression. Primer sequences were presented in Tables S1 and S2 (ESI[†]).

2.9 Target gene prediction and pathway analysis

The OmicStudio (<https://www.omicstudio.cn/analysis/targetGene>) is an operation shell linking to API from TargetScan and miRanda Target Prediction Database, which was used to identify EVs-miRNAs targets. These target genes were uploaded into Metascape to provide a comprehensive biological pathways enrichment analysis.³⁵ The identified terms were visualized through ggplot2 package in R.

2.10 Statistical analysis

The data were analyzed using GraphPad Prism 8.0.2 and IBM SPSS Statistics 26.0. All data were represented as mean ± SEM. Student's *t*-test and one-way ANOVA analysis with the Tukey multiple comparison test were used to confirm statistical significance. The correlations between miRNA expression levels and myoglobin (MYO), Creatine Kinase-MB (CK-MB), Global Registry of Acute Coronary Events (GRACE) Score, cardiac troponins T (cTnT) and N-terminal pro-B natriuretic peptide (NT-proBNP) were assessed by Spearman's correlation analysis. The receiver operating characteristic (ROC) curve was constructed using each miRNA relative expression value individually on the website (<https://www.bioinformatics.com.cn/>). *P* value < 0.05 was considered statistically significant.

3 Results

3.1 Baseline characteristics of the study population

Table 1 summarizes the baseline characteristics of the 9 SCD patients and 9 matched HC in testing groups. Every 3 samples were randomly and equally mixed and used for miRNA sequencing. The clinical characteristics of the 30 SCD patients and 30 HC are summarized in Table 2. As shown, no statistical significance was observed between the two groups with regard to age, gender, body mass index (BMI), previous histories and platelet (PLT). However, levels of WBC count, CK-MB, cTnT, MYO, NT-proBNP and aspartate transaminase (AST) of the patients in the SCD group were markedly higher than the normal value. Killip class of patients in the SCD group was absolutely divided into I–IV levels. In addition, the mean \pm SD GRACE score of the SCD group was 219.3 ± 21.5 in testing participants and 217.9 ± 32.4 in validating participants.

3.2 Characterization of isolated EVs in plasma

The flow chart in Fig. 1A shows the procedure of isolating EVs from the plasma by ultracentrifugation. EVs in the HC group and the SCD group were identified by TEM and NTA measurements, respectively. Western blotting was carried out to assess the positive protein markers CD9, CD63, CD81, HSP70 and the negative marker calnexin (Fig. 1B). Whole plasma was used as a positive control. As shown in Fig. 1C, the EVs extracted from plasma were fully purified and displayed round-shaped, vesicle-like structures under the TEM in both the SCD group and the HC group. The concentration and size distribution of the isolated EVs are shown in Fig. 1D, which revealed that the diameters of EVs were predominantly < 150 nm and corresponded to the typical diameter of EVs. All above results indicated that the EVs were fully purified.

Table 2 The baseline data of the validated participants

Characteristics	HC	SCD	P value
Sample size	30	30	—
Age (y)	58.6 ± 11.4	58.1 ± 13.5	0.8936
Male (%)	23 (76.7)	24 (80)	1.0000
BMI (kg m^{-2})	25.0 ± 3.3	25.0 ± 2.7	0.9757
Smoking (%)	13 (43.3)	13 (43.3)	1.0000
Hypertension (%)	17 (56.7)	19 (63.3)	0.7925
Diabetes (%)	2 (6.7)	6 (20)	0.2542
Hyperlipidemia (%)	4 (13.3)	3 (10)	1.0000
Killip class (%)			
I	—	1 (3.3)	—
II	—	5 (16.7)	—
III	—	2 (6.7)	—
IV	—	22 (73.3)	—
Grace score	—	217.9 ± 32.4	—
WBC ($\times 10^9/\text{L}$)	6.6 ± 1.6	15.5 ± 6.7	< 0.0001
PLT ($\times 10^9/\text{L}$)	231 ± 48.0	215 ± 166.7	0.6153
CK-MB (ng mL^{-1})	—	102.4 ± 120.1	—
cTnT (ng mL^{-1})	—	3600.2 ± 3762.1 ($n = 29$)	—
MYO (ng mL^{-1})	—	681.7 ± 965.2	—
NT-proBNP (pg mL^{-1})	—	3476.2 ± 6805.6 ($n = 29$)	—
AST (U L^{-1})	25 ± 11.0	449.4 ± 629.7 ($n = 29$)	0.0005

HC, healthy control; SCD, sudden cardiac death; BMI, Body Mass Index; WBC, white blood cell; PLT, platelet; CK-MB, Creatine Kinase-MB; cTnT, troponin T; MYO, myoglobin; NT-proBNP, N-terminal pro-B natriuretic peptide; AST, Aspartate Transaminase.

3.3 MiRNA profile of plasma EVs by sequencing

Initially, a total of 1363 hsa-miRNAs were found in plasma EVs of the 9 SCD patients and 9 HC by miRNA sequencing. A total of 111 miRNAs showed a significant difference between the two groups after filtering (Table S3, ESI†). Of these, 55 miRNAs were upregulated, and 56 miRNAs were downregulated. The heatmap in Fig. 2A displays the patterns of miRNA expression between the two experimental groups after filtering. The

Table 1 Comparison of clinical characteristics between the testing HC group and SCD group

Characteristics	HC	SCD	P value
Sample size	9	9	—
Age (y)	49.4 ± 6.8	49.6 ± 5.3	0.9697
Male (%)	9 (100)	9 (100)	1.0000
BMI (kg m^{-2})	25.8 ± 2.5	26.5 ± 2.6	0.5822
Smoking (%)	6 (66.7)	5 (55.6)	1.0000
Hypertension (%)	1 (11.1)	5 (55.6)	0.1300
Diabetes (%)	0 (0)	2 (22.2)	0.4700
Hyperlipidemia (%)	0 (0)	0 (0)	1.0000
Killip class (%)			
I	—	0 (0)	—
II	—	0 (0)	—
III	—	0 (0)	—
IV	—	9 (100)	—
Grace score	—	219.3 ± 21.5	—
WBC ($\times 10^9/\text{L}$)	6.6 ± 2.0	16.3 ± 6.0 ($n = 8$)	0.0004
PLT ($\times 10^9/\text{L}$)	199.8 ± 95.4	202.8 ± 92.5 ($n = 8$)	0.9499
CK-MB (ng mL^{-1})	—	74.5 ± 105.7 ($n = 5$)	—
cTnT (ng mL^{-1})	—	4309.8 ± 4692.8 ($n = 9$)	—
MYO (ng mL^{-1})	—	1326.3 ± 1397.4 ($n = 8$)	—
NT-proBNP (pg mL^{-1})	—	237.8 ± 146.2 ($n = 8$)	—
AST (U L^{-1})	24.4 ± 5.4 ($n = 9$)	425.1 ± 283.2 ($n = 9$)	0.0006

HC, healthy control; SCD, sudden cardiac death; BMI, body mass index; WBC, white blood cell; PLT, platelet; CK-MB, creatine kinase-MB; cTnT, troponin T; MYO, myoglobin; NT-proBNP, N-terminal pro-B natriuretic peptide; AST, aspartate transaminase.

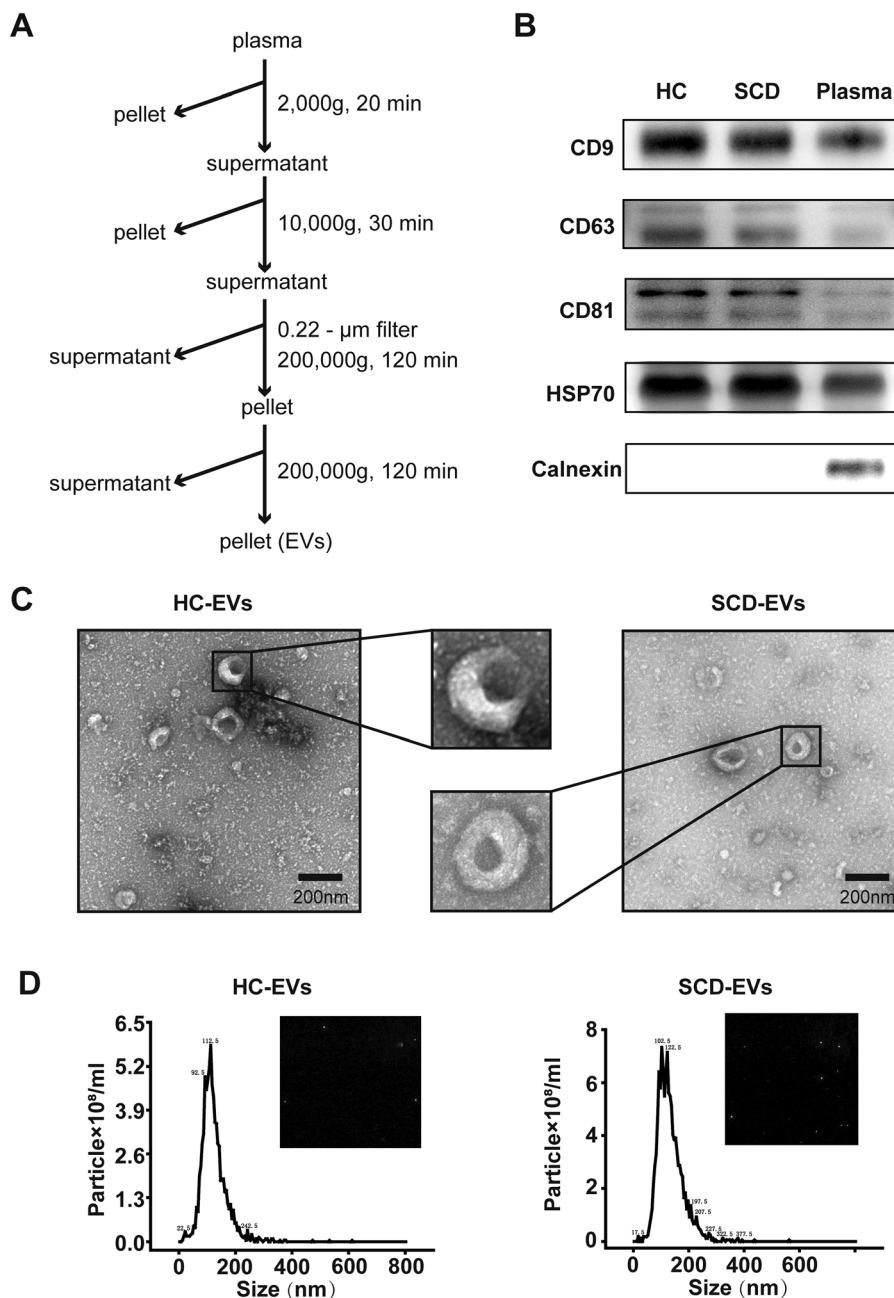


Fig. 1 Working flow of EVs isolation from plasma and characterization of EVs. (A) The procedure of isolating EVs from the plasma by ultracentrifugation. (B) Western blotting of EVs markers (positive markers CD9, CD63, CD81, HSP70 and negative marker calnexin). (C) TEM images of extracted EVs from HC and SCD group; scale bar = 200 nm. NTA measurements of EVs extracted from HC and SCD group. EVs, extracellular vesicles; TEM, transmission electron microscope; HC, healthy control; SCD, sudden cardiac death; NTA, nanoparticle tracking analysis.

expressions of identified miRNAs in the two groups were assessed by plotting the Log₂-ratio and volcano plot (Fig. 2B).

3.4 Confirmation of plasma EVs' miRNA expression profiles in testing groups

In consideration of the feasibility of subsequent validation, we focused on the plasma EVs miRNAs with high expression levels. To validate the accuracy and authenticity of sequencing results, the top 5 upregulated miRNAs (miR-208b-3p, miR-143-3p,

miR-145-3p, miR-145-5p and miR-152-3p) and the top 5 down-regulated miRNAs (miR-144-5p, miR-182-5p, miR-144-3p, miR-183-5p and miR-96-5p) in the SCD group compared to the HC group were further quantified in the testing groups by RT-qPCR (Fig. 2C–L). Because of the insufficient plasma volume in testing groups, we could only detect the plasma miRNAs expressions of 5 individuals in each group. Among these 10 miRNAs, miR-208b-3p, miR-143-3p and miR-145-5p were significantly upregulated. MiR-145-3p, miR-152-3p,

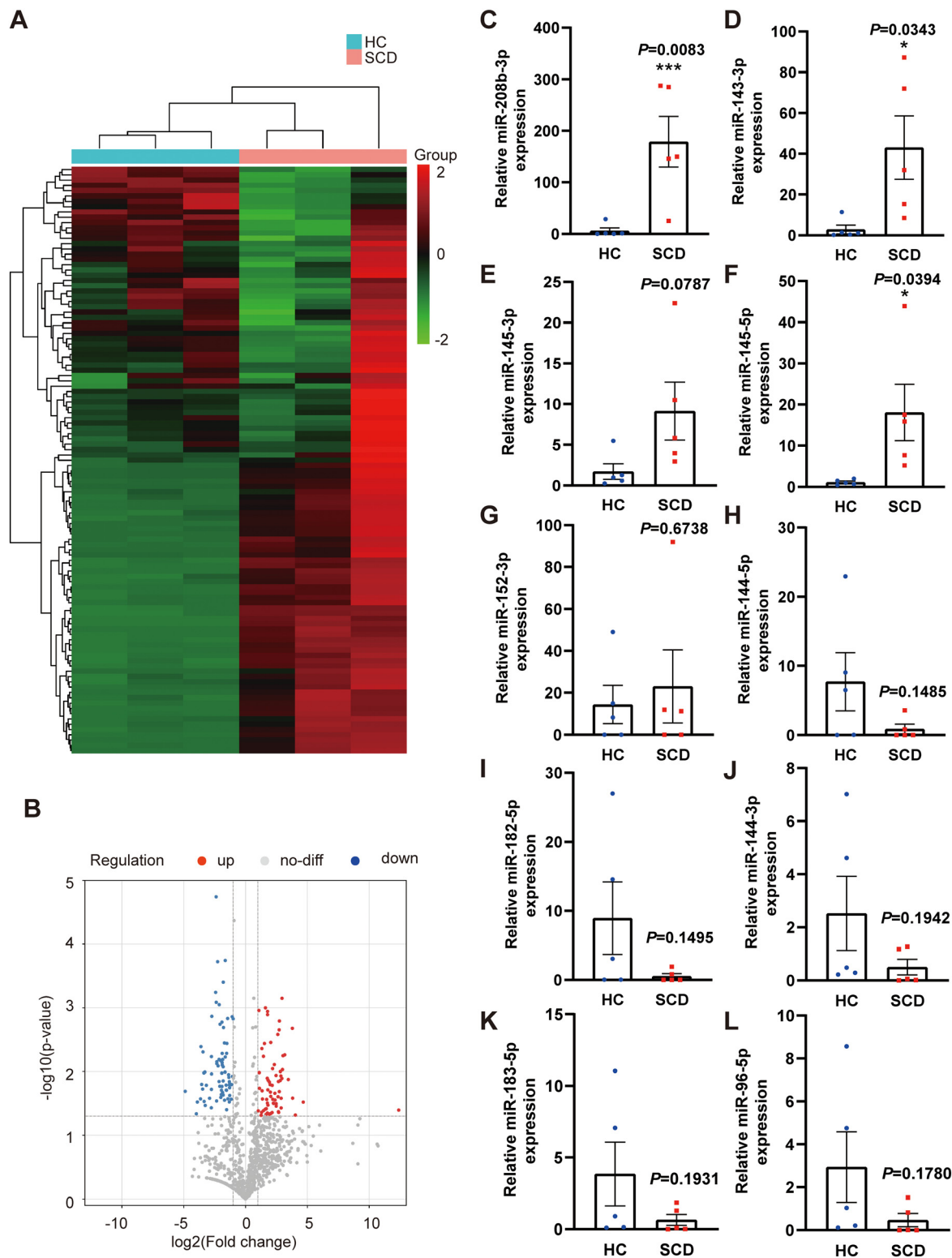


Fig. 2 The miRNA profile of plasma EVs by miRNA sequencing and the confirmation of plasma EVs-miRNA expression profiles. (A) The heatmap of differentially expressed miRNA in plasma EVs in HC ($n = 9$) and SCD ($n = 9$) group. Every three samples were randomly and equally mixed. (B) Volcano plot of miRNA expression levels in plasma EVs between HC and SCD group. The P -value together with log 2 fold change was introduced with a cutoff value of 0.05 for the P -value and 2 for log 2 FC, respectively. (C–L) RT-qPCR expression analysis of indicated miRNAs in plasma EVs from the HC group ($n = 5$) and SCD group ($n = 5$). Significance was determined by Student's t test. * $P < 0.05$, *** $P < 0.001$. All graphs are shown as mean \pm SEM. MiRNA, microRNA; EVs, extracellular vesicles; HC, healthy control; SCD, sudden cardiac death; RT-qPCR, reverse transcription and real-time quantitative polymerase chain reaction.

miR-144-5p, miR-182-5p, miR-144-3p, miR-183-5p and miR-96-5p showed no statistical difference. Table 3 shows the specific results of sequencing and RT-qPCR of the top 10 miRNAs.

3.5 Validation of differentially expressed EVs' miRNAs using samples in validation groups

To further validate the values of the selected top 10 differentially expressed miRNAs as potential biomarkers, 30 SCD patients and 30 HC were enrolled in the validation group. As shown in Fig. 3A–E, the expression levels of plasma EVs miR-208b-3p, miR-143-3p, miR-145-3p and miR-152-3p were significantly upregulated in SCD group compared to HC group, and miR-183-5p was significantly downregulated in SCD group compared to HC group by RT-qPCR. The results were consistent with the miRNA sequencing results. The expression levels of the other five miRNAs showed no statistical significance (Fig. S1, ESI[†]).

3.6 Correlations between clinical indicators and levels of plasma EVs' miRNAs

We assessed the correlations between the expression levels of validated plasma EVs miR-208b-3p, miR-143-3p, miR-145-3p, miR-152-3p, miR-183-5p and MYO, CK-MB, GRACE Score, cTnT, NT-proBNP by Spearman's correlation analysis, respectively. Plasma EVs miR-208b-3p level was not related to GRACE Score ($r = 0.3$, $P = 0.1$), CK-MB ($r = 0.36$, $P = 0.051$), cTnT ($r = 0.17$, $P = 0.38$) or NT-proBNP ($r = -0.002$, $P = 0.99$) in SCD patients (Fig. 3F–G, supplemental Fig. S2A and B, ESI[†]). As shown in Fig. 3H, plasma EVs miR-208b-3p level was positively correlated with MYO ($r = 0.46$, $P = 0.011$) in SCD patients. Plasma EVs miR-143-3p level had no relation with GRACE Score ($r = 0.35$, $P = 0.059$), CK-MB ($r = 0.36$, $P = 0.052$), cTnT ($r = 0.17$, $P = 0.37$) and NT-proBNP ($r = 0.081$, $P = 0.68$) in SCD patients (Fig. 3I and J, Fig. S2C and D, ESI[†]) and was positively correlated with MYO ($r = 0.47$, $P = 0.0092$) (Fig. 3K). We also evaluated the correlations between plasma EVs miR-145-3p, miR-152-3p and miR-183-5p and the above 5 clinical indicators, which showed no statistical significance.

3.7 Evaluation of the diagnostic effects of Plasma EVs miRNAs

To determine the discriminatory power of the plasma EVs miR-208b-3p and miR-143-3p, we plotted ROC curves (Fig. 3L). The

AUC for miR-208b-3p was 0.7756 and that for miR-143-3p was 0.7778, indicating fair predictive power. The above results indicated that miR-208b-3p and miR-143-3p in plasma EVs may serve as biomarkers for predicting SCD.

3.8 The functional enrichment of miR-208b-3p and miR-143-3p targets

Based on predicted target genes of miR-208b-3p and miR-143-3p, functional enrichment analyses were performed. Significant biological process and pathways regulated by miR-208b-3p were obtained (Fig. 4A), including heart valve formation, regulation of cardiac muscle cell contraction, and regulation of cardiac muscle cell action potential. MiR-143-3p was involved in the negative regulation of cardiac muscle contraction, cardiac muscle hypertrophy in response to stress, cardiac muscle adaptation, cardiac muscle cell apoptotic process and regulation of cardiac muscle cell action potential, *etc.* (Fig. 4B). GO, KEGG, Reactome and wiki database were used, but some of the pathways enriched by miR-143-3p targets did not pass the significance criteria, thus only pathways from GO and wiki database are shown in Fig. 4B. The corresponding data including q value, enrichment value, P value and so on are listed in Table S4 (ESI[†]).

4 Discussion

In our present study, plasma EVs of 39 ACS patients experiencing SCD and 39 HC were isolated and purified by ultracentrifugation and subsequently characterized by NTA, TEM and Western blotting. Nine samples from each group were randomly selected for miRNA sequencing to obtain specific plasma EVs miRNA biomarkers of SCD. Every 3 samples were randomly and equally mixed and used for miRNA sequencing. The miRNA sequencing results comprised statistically significantly increased miR-208b-3p, miR-143-3p, miR-145-3p, miR-145-5p, and miR-152-3p with decreased miR-144-5p, miR-182-5p, miR-144-3p, miR-183-5p and miR-96-5p. To further validate the values of the selected top 10 differentially expressed miRNAs as potential biomarkers, 30 SCD patients and 30 HC were enrolled in the validation group. Of these 10 miRNAs, miR-208b-3p, miR-143-3p, miR-145-3p and miR-152-3p were significantly upregulated and miR-183-5p was

Table 3 The relative expression level of the top 10 expressed microRNAs selected for validation

Index	Sequencing result					RT-qPCR result		
	Name	Up/down	Fold change	Log2(fold change)	P value	Up/down	Fold change	P value
1	miR-208b-3p	Up	5376.57	12.39	0.0402	Up	28.57	0.0083
2	miR-143-3p	Up	13.82	3.79	0.0021	Up	14.90	0.0343
3	miR-145-3p	Up	10.99	3.46	0.0133	Up	5.32	0.0787
4	miR-145-5p	Up	7.35	2.88	0.0262	Up	15.80	0.0394
5	miR-152-3p	Up	6.30	2.66	0.0143	Up	1.59	0.6738
6	miR-144-5p	Down	0.07	−3.74	<0.0001	Down	0.16	0.1485
7	miR-182-5p	Down	0.08	−3.64	0.0268	Down	0.06	0.1495
8	miR-144-3p	Down	0.09	−3.47	0.0188	Down	0.20	0.1942
9	miR-183-5p	Down	0.10	−3.37	0.0105	Down	0.17	0.1931
10	miR-96-5p	Down	0.15	−2.77	0.0370	Down	0.16	0.1780

miRNA, microRNA; RT-qPCR, real-time quantitative polymerase chain reaction.

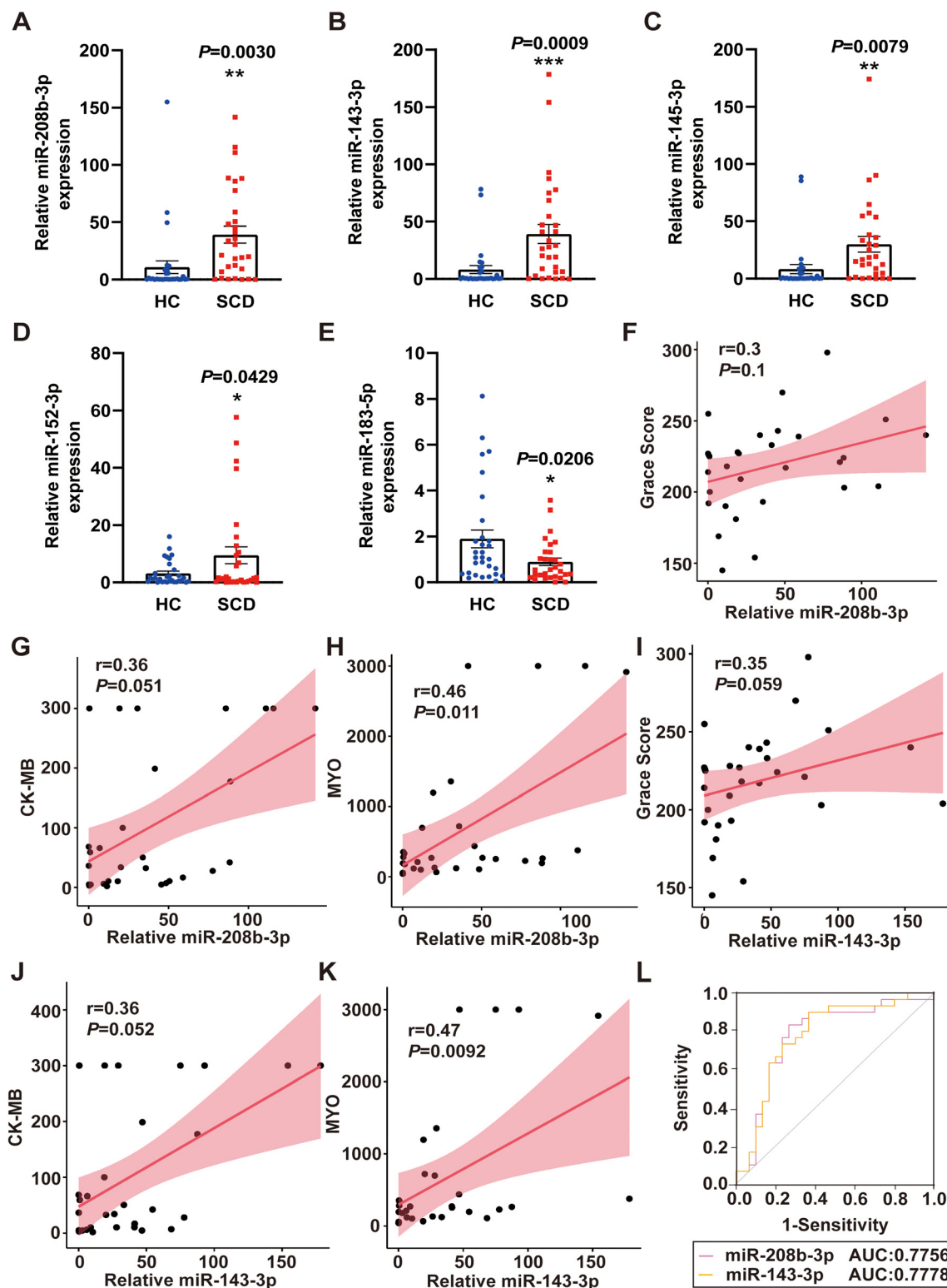


Fig. 3 Validation of miRNAs in plasma EVs and correlation between ACS relevant clinical indicators and plasma EVs miRNAs. (A–E) RT-qPCR expression analysis of miR-208b-3p, miR-143-3p, miR-145-3p, miR-152-3p and miR-183-5p in plasma EVs from HC ($n = 30$) and SCD ($n = 30$) group in the validation group. Significance was determined by Student's t test. $*P < 0.05$, $**P < 0.01$, $***P < 0.001$. (F–K) Correlations between ACS relevant clinical indicators (Grace score, CK-MB and MYO) and plasma EVs miR-208b-3p and miR-143-3p. Significance was determined by Spearman's correlation analysis. $P < 0.05$ was considered statistically significant. (L) The ROC curves of plasma EVs miR-208b-3p and miR-143-3p with the AUC value of 0.7756 for miR-208b-3p and 0.7778 for miR-143-3p. All graphs are shown as mean \pm SEM. MiRNA, microRNA; EVs extracellular vesicles; ACS, acute coronary syndrome; RT-qPCR, reverse transcription and real-time quantitative polymerase chain reaction; HC, healthy control; SCD, sudden cardiac death; CK-MB, creatine kinase-MB; MYO, myoglobin; ROC, receiver operating characteristic.

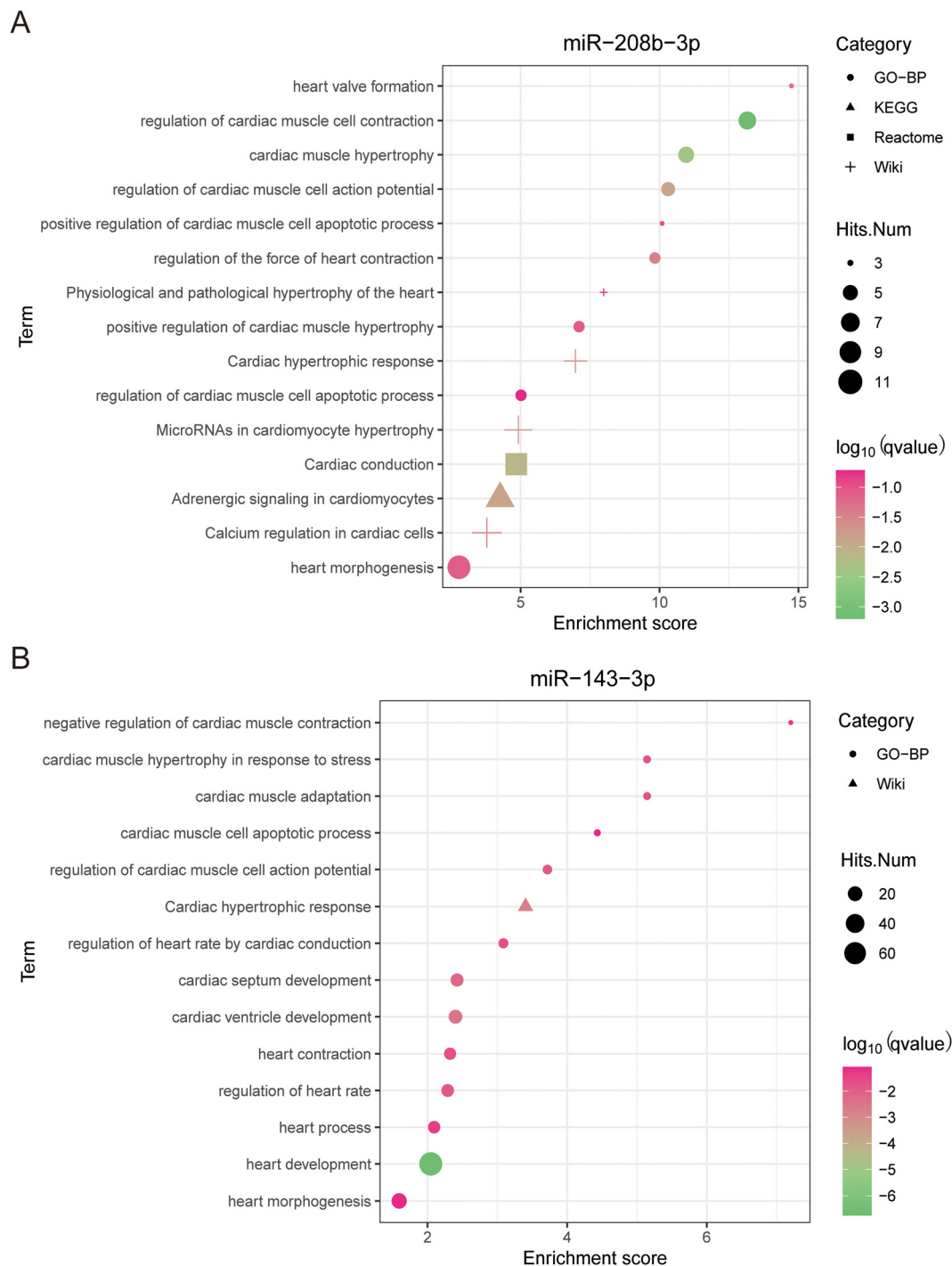


Fig. 4 The functional enrichment of miR-208b-3p and miR-143-3p targets.

significantly downregulated between the two groups. By Spearman's correlation analysis and ROC analysis, miR-208b-3p and miR-143-3p were identified to be potential biomarkers for predicting SCD in ACS patients. The comprehensive biological pathways enrichment analysis showed that the regulated genes and pathways, including heart valve formation, regulation of cardiac muscle cell contraction, regulation of cardiac muscle cell action potential, were dysregulated by miR-208b-3p, which were all critical for cardiac pacing. MiR-143-3p was involved in negative

regulation of cardiac muscle contraction, cardiac muscle hypertrophy in response to stress, cardiac muscle adaptation, cardiac muscle cell apoptotic process and regulation of cardiac muscle cell action potential, *etc.*

We choose EVs isolated from plasma as our samples because EVs miRNAs are thought to be more specific and sensitive biomarkers, given that EVs are secreted into extracellular space in a selective approach when compared with free miRNAs or total cellular miRNAs.³⁶ Certain miRNA biomarkers of EVs can

reflect the characteristics of their parent cells.³⁷ Besides, EVs are remarkably stable in biofluids, such as plasma and urine.²⁰ Therefore, EVs are considered to be ideal diagnostic biomarker carriers. The above advantages make EVs superior to whole serum for screening biomarkers.^{21,37} Here, in this study, we focused on the miRNA profile of plasma EVs from ACS patients experiencing SCD to screen for biomarkers to predict SCD.

According to our findings, plasma EV miR-208b-3p was significantly upregulated in ACS patients experiencing SCD *versus* HC and the finding was in line with previous studies. Previous study showed that there was a statistically significant increase of circulating miR-208b-3p in ACS patients when compared with cerebral ischaemic event (CIE) patients.³⁸ Hypoxia/reoxygenation (HR) increased the expression of miR-208b-3p, and inhibition of miR-208b-3p had a protective influence on H9c2 cells against HR injury by negatively regulating Med13 expression and aggravating HR injury through the Wnt/ β -catenin signaling pathway.³⁹ Plasma expression of miR-208b in MI patients was significantly upregulated with respect to healthy individuals,⁴⁰ which was consistent with our results. To our best knowledge, miR-208b-3p has not been studied in plasma EVs from ACS patients experiencing SCD. Combined with the ROC curve, we found that miR-208b-3p (AUC = 0.7756) showed the superior potency to predict SCD.

Besides miR-208b-3p, plasma EV miR-143-3p was significantly upregulated in ACS patients experiencing SCD *versus* HC in our results. MiR-143-3p is related to cardiovascular diseases and has been found to be observably upregulated in the myocardium after MI in the infarct zone of human MI samples. MiR-143-3p, along with SPRY3, regulates biological functions *via* the activation of p38, ERK, and JNK pathways.⁴¹ MiR-143-3p is found to be upregulated in the rabbit CHD model and associated with cell viability, apoptosis and migration of vascular smooth muscle cells by targeting killin (KLLN).⁴² Melatonin regulates cardiomyocyte proliferation and cardiac regeneration after MI *via* the Yap/Ctnd1 signaling pathway, which are regulated by miR-143-3p.⁴³ In addition, suppressing the miR-143-3p expression level can protect myocardial ischemia-reperfusion (I/R) injury by activating the AMPK/Foxo1 pathway.⁴⁴ We compared the hsa-miR-143 expression profile of EVs with the reported profile of plasma. Interestingly, hsa-miR-143 showed an inverse expression pattern when measured in the plasma.⁴⁵

To assess the relationships of the identified plasma EVs miRNAs with clinical features, MYO, CK-MB, cTnT, NT-proBNP and GRACE Score were selected, which were widely used clinical indicators in ACS diagnosis.⁴⁶ MYO exists in heart and striated skeletal muscle and is released rapidly after myocardial injury but is less cardiospecific than CK-MB and cTnT.⁴⁷ CK-MB and cTnT have been taken as sensitive and specific biomarkers of myocyte necrosis.⁴⁸ NT-proBNP is secreted from the heart, resulting from myocyte stretch, endocrine activation, and myocardial hypoxia.⁴⁹ GRACE Score is the preferred scoring system for risk stratification in ACS and can be used to predict the risk of death.^{50,51} By Spearman's correlation analysis, both plasma EVs miR-208b-3p and miR-143-3p levels were positively correlated with MYO in SCD patients,

respectively, indicating their potential functions during the progression of myocardial injury.

To date, identification of the cause of death in SCD cases also remains one of the most challenging subjects in forensic practice due to the lack of biomarkers.⁴ Previous studies have shown that it is feasible to isolate EVs from post-mortem body fluids, and EVs RNAs are well-preserved, which could be used for forensic diagnosis.⁵² It has been considered that miRNAs in EVs play an important role in cardiovascular diseases and may be able to provide objective evidence of SCD identification in forensic diagnosis.⁵³ In our study, we found that miR-208b-3p and miR-143-3p in EVs derived from plasma were significantly upregulated in ACS patients experiencing SCD compared with HC. The measurement of biomarkers in EVs on forensic biopsy will be performed in our future studies. We hope our work will provide a novel aspect for forensic researchers.

We did acknowledge several limitations to our work: (1) the sample size of our study was relatively limited, while a larger sample size would be more credible. However, though we tried our best to collect samples, it was challenging to exclude non-cardiac causes of death, particularly when autopsies were not routinely performed in the hospital. Nevertheless, interrogation of the available data still provided new insights into SCD epidemiology both for SCD prediction in ACS patients and forensic investigation. (2) Lack of the clinical indicators' information of healthy people made it difficult to compare the ROC for the two miRNAs and the cardiac biomarkers including MYO, CK-MB, cTnT, GRACE Score and NT-proBNP. (3) The mechanism was not clearly established on the identified miRNAs, which was the direction that needs further exploration in the future.

In conclusion, this study indicated that expression levels of plasma EVs miR-208b-3p and miR-143-3p were significantly increased in ACS patients experiencing SCD, thus might be identified as novel biomarkers for predicting SCD in patients with ACS. Overall, our results may provide new insights for clinical prevention and management of SCD, and expand the scope of miRNA application in forensic science.

Data availability

The raw sequence data reported in this article have been deposited in the Genome Sequence Archive⁵⁴ in the National Genomics Data Center,⁵⁵ China National Center for Bioinformation/Beijing Institute of Genomics, Chinese Academy of Sciences (GSA-Human: HRA003509) that are publicly accessible at <https://ngdc.cncb.ac.cn/gsa-human>.

Author contributions

Shuainan Huang, Jiahui Zhang and Hua Wan performed experiments. Youjia Yu, Jinsong Zhang, Jie Wang, and Feng Chen designed the experiments. Jiayi Wu, Yue Cao, Li Hu, Yanfang Yu and Hao Sun collected the plasma samples and performed critical reading/editing of the manuscript. Shuainan

Huang, Kang Wang, Youjia Yu, Jie Wang, and Feng Chen wrote the manuscript.

Conflicts of interest

The authors declare that they have no conflict of interest.

Acknowledgements

This work was supported by the National Natural Science Foundation of China (No. 82225023, No. 81922041, and No. 82121001), the Open Project of State Key Laboratory of Cardiovascular Diseases (SKL2021019), the China Postdoctoral Science Foundation (2021M701758), and the Postdoctoral Research Project of Gusu School of Nanjing Medical University (GSBSHKY202103).

References

- 1 M. W. Deyell, A. D. Krahn and J. J. Goldberger, *Circ. Res.*, 2015, **116**, 1907–1918.
- 2 J. S. Lucena, *Forensic. Sci. Res.*, 2019, **4**, 199–201.
- 3 P. Markwerth, T. Bajanowski, I. Tzimas and R. Dettmeyer, *Int. J. Legal. Med.*, 2021, **135**, 483–495.
- 4 J. Lou, H. Chen, S. Huang, P. Chen, Y. Yu and F. Chen, *J. Forensic Leg. Med.*, 2022, **87**, 102332.
- 5 Y. T. Feng and X. F. Feng, *Rev. Cardiovasc. Med.*, 2021, **22**, 807–816.
- 6 M. Pouralijan Amiri, M. Khoshkam, R. M. Salek, R. Madadi, G. Faghanzadeh Ganji and A. Ramazani, *Clin. Chim. Acta*, 2019, **495**, 43–53.
- 7 F. Sanchis-Gomar, C. Perez-Quilis, R. Leischik and A. Lucia, *Ann. Transl. Med.*, 2016, **4**, 256.
- 8 F. Lin, Y. Yang, Q. Guo, M. Xie, S. Sun, X. Wang, D. Li, G. Zhang, M. Li, J. Wang and G. Zhao, *J. Evidence-Based Complementary Altern. Med.*, 2020, **2020**, 1584052.
- 9 W. Zhang, G. Chang, L. Cao and G. Ding, *BMC Cardiovasc. Disord.*, 2021, **21**, 74.
- 10 D. D. Taylor and C. Gercel-Taylor, *Gynecol. Oncol.*, 2008, **110**, 13–21.
- 11 J. M. Vicencio, D. M. Yellon, V. Sivaraman, D. Das, C. Boi-Doku, S. Arjun, Y. Zheng, J. A. Riquelme, J. Kearney, V. Sharma, G. Multhoff, A. R. Hall and S. M. Davidson, *J. Am. Coll. Cardiol.*, 2015, **65**, 1525–1536.
- 12 L. J. Li, Y. J. Gu, L. Q. Wang, W. Wan, H. W. Wang, X. N. Yang, L. L. Ma, L. H. Yang and Z. H. Meng, *J. Thorac. Dis.*, 2021, **13**, 3105–3114.
- 13 K. S. Yang, H. Im, S. Hong, I. Pergolini, A. F. Del Castillo, R. Wang, S. Clardy, C. H. Huang, C. Pille, S. Ferrone, R. Yang, C. M. Castro, H. Lee, C. F. Del Castillo and R. Weissleder, *Sci. Transl. Med.*, 2017, **9**, eaal3226.
- 14 A. Hoshino, H. S. Kim, L. Bojmar, K. E. Gyan, M. Cioffi, J. Hernandez, C. P. Zambirinis, G. Rodrigues, H. Molina, S. Heissel, M. T. Mark, L. Steiner, A. Benito-Martin, S. Lucotti, A. Di Giannatale, K. Offer, M. Nakajima, C. Williams, L. Nogués, F. A. Pellissier Vatter, A. Hashimoto, A. E. Davies, D. Freitas, C. M. Kenific, Y. Ararso, W. Buehring, P. Lauritzen, Y. Ogitani, K. Sugiura, N. Takahashi, M. Alečković, K. A. Bailey, J. S. Jolissant, H. Wang, A. Harris, L. M. Schaeffer, G. García-Santos, Z. Posner, V. P. Balachandran, Y. Khakoo, G. P. Raju, A. Scherz, I. Sagi, R. Scherz-Shouval, Y. Yarden, M. Oren, M. Malladi, M. Petriccione, K. C. De Braganca, M. Donzelli, C. Fischer, S. Vitolano, G. P. Wright, L. Ganshaw, M. Marrano, A. Ahmed, J. DeStefano, E. Danzer, M. H. A. Roehrl, N. J. Lacayo, T. C. Vincent, M. R. Weiser, M. S. Brady, P. A. Meyers, L. H. Wexler, S. R. Ambati, A. J. Chou, E. K. Slotkin, S. Modak, S. S. Roberts, E. M. Basu, D. Diolaiti, B. A. Krantz, F. Cardoso, A. L. Simpson, M. Berger, C. M. Rudin, D. M. Simeone, M. Jain, C. M. Ghajar, S. K. Batra, B. Z. Stanger, J. Bui, K. A. Brown, V. K. Rajasekhar, J. H. Healey, M. de Sousa, K. Kramer, S. Sheth, J. Baisch, V. Pascual, T. E. Heaton, M. P. La Quaglia, D. J. Pisapia, R. Schwartz, H. Zhang, Y. Liu, A. Shukla, L. Blavier, Y. A. DeClerck, M. LaBarge, M. J. Bissell, T. C. Caffrey, P. M. Grandgenett, M. A. Hollingsworth, J. Bromberg, B. Costa-Silva, H. Peinado, Y. Kang, B. A. Garcia, E. M. O'Reilly, D. Kelsen, T. M. Trippett, D. R. Jones, I. R. Matei, W. R. Jarnagin and D. Lyden, *Cell*, 2020, **182**, 1044–1061.
- 15 L. Zhu, Y. Xu, S. Kang, B. Lin, C. Zhang, Z. You, H. Lin, C. Yang and Y. Song, *Small Methods*, 2022, **6**, e2200549.
- 16 S. Mirzaei, M. D. A. Paskeh, E. Okina, M. H. Gholami, K. Hushmandi, M. Hashemi, A. Kalu, A. Zarrabi, N. Nabavi, N. Rabiee, E. Sharifi, H. Karimi-Maleh, M. Ashrafizadeh, A. P. Kumar and Y. Wang, *J. Exp. Clin. Cancer Res.*, 2022, **41**, 214.
- 17 X. Zheng, J. L. Carstens, J. Kim, M. Scheible, J. Kaye, H. Sugimoto, C. C. Wu, V. S. LeBleu and R. Kalluri, *Nature*, 2015, **527**, 525–530.
- 18 J. Lin, J. Li, B. Huang, J. Liu, X. Chen, X. M. Chen, Y. M. Xu, L. F. Huang and X. Z. Wang, *Sci. World J.*, 2015, **2015**, 657086.
- 19 Y. Kuwabara, K. Ono, T. Horie, H. Nishi, K. Nagao, M. Kinoshita, S. Watanabe, O. Baba, Y. Kojima, S. Shizuta, M. Imai, T. Tamura, T. Kita and T. Kimura, *Circ.: Cardiovasc. Genet.*, 2011, **4**, 446–454.
- 20 H. Ling, Z. Guo, Y. Shi, L. Zhang and C. Song, *Front. Physiol.*, 2020, **11**, 654.
- 21 K. O'Brien, K. Breyne, S. Ughetto, L. C. Laurent and X. O. Breakefield, *Nat. Rev. Mol. Cell Biol.*, 2020, **21**, 585–606.
- 22 D. Santovito and C. Weber, *Eur. Heart J.*, 2017, **38**, 524–528.
- 23 J. R. Zibert, M. B. Løvendorf, T. Litman, J. Olsen, B. Kaczkowski and L. Skov, *J. Dermatol. Sci.*, 2010, **58**, 177–185.
- 24 J. Beermann, M. T. Piccoli, J. Viereck and T. Thum, *Physiol. Rev.*, 2016, **96**, 1297–1325.
- 25 R. Bai, Q. Yang, R. Xi, L. Li, D. Shi and K. Chen, *BMC Cardiovasc. Disord.*, 2017, **17**, 227.
- 26 R. Szelenberger, M. S. Karbownik, M. Kacprzak, K. Maciak, M. Bijak, M. Zielińska, P. Czarny, T. Śliwiński and J. Saluk-Bijak, *Cells*, 2021, **10**, 3526.
- 27 M. G. Silverman, A. Yeri, M. V. Moorthy, F. Camacho Garcia, N. A. Chatterjee, C. S. A. Glinge, J. Tfelt-Hansen, A. M. Salvador,

- A. R. Pico, R. Shah, C. M. Albert and S. Das, *JACC: Clin. Electrophysiol.*, 2020, **6**, 70–79.
- 28 Z. Yang, Q. Zhang, H. Yu, H. Du, L. Li, Y. He, S. Zhu, C. Li, S. Zhang, B. Luo and Y. Gao, *Forensic Sci. Int.*, 2021, **318**, 110637.
- 29 F. Yan, Y. Chen, X. Ye, F. Zhang, S. Wang, L. Zhang and X. Luo, *Diagn. Pathol.*, 2021, **16**, 67.
- 30 J. Boere, C. H. A. van de Lest, J. C. de Grauw, S. G. M. Plomp, S. Libregts, G. J. A. Arkesteijn, J. Malda, M. H. M. Wauben and P. R. van Weeren, *Vet. J.*, 2019, **244**, 91–93.
- 31 F. Guan, X. Xiang, Y. Xie, H. Li, W. Zhang, Y. Shu, J. Wang and W. Qin, *Anal. Methods*, 2021, **13**, 1930–1938.
- 32 Q. X. Chen, W. P. Wang, S. Zeng, S. Urayama and A. M. Yu, *Nucleic Acids Res.*, 2015, **43**, 3857–3869.
- 33 Y. Song, X. An, L. Zhang, M. Fu, J. Peng, P. Han, J. Hou, Z. Zhou and B. Cao, *PLoS One*, 2015, **10**, e0122202.
- 34 C. M. Ward, T. H. To and S. M. Pederson, *Bioinformatics*, 2020, **36**, 2587–2588.
- 35 Y. Zhou, B. Zhou, L. Pache, M. Chang, A. H. Khodabakhshi, O. Tanaseichuk, C. Benner and S. K. Chanda, *Nat. Commun.*, 2019, **10**, 1523.
- 36 Y. Chen, Y. Song, J. Huang, M. Qu, Y. Zhang, J. Geng, Z. Zhang, J. Liu and G. Y. Yang, *Front. Neurol.*, 2017, **8**, 57.
- 37 Z. Y. Wang, B. X. Yan, Y. Zhou, X. Y. Chen, J. Zhang, S. Q. Cai, M. Zheng and X. Y. Man, *J. Invest. Dermatol.*, 2021, **141**(185–189), e184.
- 38 J. Gacoń, R. Badacz, E. Stępień, I. Karch, F. J. Enguita, K. Żmudka, T. Przewłocki and A. Kablak-Ziembicka, *Kardiolog. Pol.*, 2018, **76**, 362–369.
- 39 Z. Wang, Y. Yang, W. Xiong, R. Zhou, N. Song, L. Liu and J. Qian, *Biomed. Pharmacother.*, 2020, **125**, 110001.
- 40 O. Gidlöf, J. G. Smith, K. Miyazu, P. Gilje, A. Spencer, S. Blomquist and D. Erlinge, *BMC Cardiovasc. Disord.*, 2013, **13**, 12.
- 41 C. Li, J. Li, K. Xue, J. Zhang, C. Wang, Q. Zhang, X. Chen, C. Gao, X. Yu and L. Sun, *J. Mol. Cell. Cardiol.*, 2019, **129**, 281–292.
- 42 H. Liu, W. Xiong, F. Liu, F. Lin, J. He, C. Liu, Y. Lin and S. Dong, *Am. J. Transl. Res.*, 2019, **11**, 3610–3619.
- 43 W. Y. Ma, R. J. Song, B. B. Xu, Y. Xu, X. X. Wang, H. Y. Sun, S. N. Li, S. Z. Liu, M. X. Yu, F. Yang, D. Y. Ye, R. Gong, Z. B. Han, Y. Yu, D. Bamba, N. Wang, Z. W. Pan and B. Z. Cai, *Acta Pharmacol. Sin.*, 2021, **42**, 921–931.
- 44 L. Chang, R. Shi, X. Wang and Y. Bao, *BioFactors*, 2020, **46**, 432–440.
- 45 L. Meng, X. Yu, H. Han, X. Jia, B. Hu, L. Zhang, Z. Wang, W. Zhang, M. Zhong and H. Zhu, *Clin. Biochem.*, 2023, **111**, 32–40.
- 46 L. Wang and Y. Jin, *BioMed Res. Int.*, 2020, **2020**, 3298696.
- 47 E. Danese and M. Montagnana, *Ann. Transl. Med.*, 2016, **4**, 194.
- 48 A. Yilmaz, K. Yalta, O. O. Turgut, M. B. Yilmaz, A. Ozyol, O. Kendirlioglu, F. Karadas and I. Tandogan, *Adv. Ther.*, 2006, **23**, 1060–1067.
- 49 C. Hall, *J. Card. Failure*, 2005, **11**, S81–S83.
- 50 N. Syyli, M. Hautamäki, K. Antila, S. Mahdiani, M. Eskola, T. Lehtimäki, K. Nikus, L. P. Lyytikäinen, N. Oksala and J. Hernesniemi, *Open Heart*, 2019, **6**, e001007.
- 51 K. A. Fox, G. Fitzgerald, E. Puymirat, W. Huang, K. Carruthers, T. Simon, P. Coste, J. Monsegu, P. Gabriel Steg, N. Danchin and F. Anderson, *BMJ Open*, 2014, **4**, e004425.
- 52 S. Y. Kim, S. Jang, S. Lee, J. T. Park, S. J. Lee and H. S. Kim, *Diagnostics*, 2022, **12**, 2153.
- 53 X. N. Ma, L. Lu, Y. T. Huang, C. Q. Cen, F. Y. Su, Y. Shi and Z. P. Cao, *Fayixue Zazhi*, 2022, **38**, 258–262.
- 54 T. Chen, X. Chen, S. Zhang, J. Zhu, B. Tang, A. Wang, L. Dong, Z. Zhang, C. Yu, Y. Sun, L. Chi, H. Chen, S. Zhai, Y. Sun, L. Lan, X. Zhang, J. Xiao, Y. Bao, Y. Wang, Z. Zhang and W. Zhao, *Genomics, Proteomics Bioinf.*, 2021, **19**, 578–583.
- 55 CNCB-NGDC Members and Partners, *Nucleic Acids Res.*, 2022, **50**, D27–D38.